

Electrochemical properties of amorphous $\text{Li}_x\text{V}_2\text{O}_{5-y}$ thin film deposited by r.f.-sputtering

SangDong Lee · JiYong Eom · HyukSang Kwon

Received: 1 April 2008 / Accepted: 3 September 2008 / Published online: 25 September 2008
© Springer Science+Business Media B.V. 2008

Abstract The electrochemical properties of amorphous vanadium pentoxide (V_2O_5) thin films deposited by reactive r.f.-sputtering were investigated using galvanostatic charge/discharge cycling and galvanostatic intermittent titration technique (GITT). As x in $\text{Li}_x\text{V}_2\text{O}_{5-y}$ increased ($x = 0-2.0$), the electromotive force of the lithium (Li)|1 M LiClO_4 -propylene carbonate| $\text{Li}_x\text{V}_2\text{O}_{5-y}$ cell decreased gradually without a potential plateau or an abrupt potential reduction, demonstrating that an irreversible structural change did not occur in the entire Li content. Chemical diffusivity of the Li ion in the $\text{Li}_x\text{V}_2\text{O}_{5-y}$ thin film measured using GITT was determined to be $4 \times 10^{-13}-7 \times 10^{-14} \text{ cm}^2 \text{ s}^{-1}$ in the Li content range investigated.

Keywords Vanadium oxide · Thin film Li batteries · Charge/discharge characteristics · Chemical diffusivity · Galvanostatic intermittent titration technique

1 Introduction

V_2O_5 was one of the first proposed cathode materials for rechargeable Li batteries due to its high potential of 3.5 V and high capacity of 450 mAh g^{-1} [1]. Crystalline V_2O_5 has been shown to exhibit a well-known potential plateau and an abrupt potential reduction in the charge/discharge cycle curve [2, 3]. This potential plateau and

abrupt reduction, which were associated with an irreversible structural change in the cathode, produced a significant capacity loss in the discharge process. However, a similar potential plateau and abrupt potential reduction have not been observed in amorphous V_2O_5 cathodes [4, 5].

A V_2O_5 thin film deposited by r.f.-sputtering at high O_2 pressure showed a potential plateau and abrupt potential reduction in the crystalline structure at the first discharge, but demonstrated an excellent charge/discharge property after being subjected to a structural transformation to form an amorphous structure after further discharge. This occurred because the structure of the V_2O_5 lattice broke down with Li insertion [4]. The cell reaction rate of a Li secondary battery is determined by the diffusion rate of the Li ion in the cathode as well as in the electrolyte. Thus, in order to study the cell reaction kinetics and the structural change occurring in the amorphous V_2O_5 thin film during the charge/discharge cycle, it is essential to measure the exact value of Li ion diffusivity in the amorphous V_2O_5 thin film. However, Li ion diffusivity in the amorphous V_2O_5 thin film has rarely been measured. The Li ion diffusivity in cathode materials can be measured more precisely and faster using GITT [6–9] than other techniques such as the potentiostatic method [10] or the AC impedance method [11]. This is because the cell potential, without both an IR drop in the electrolyte and the influence of the reaction at the electrolyte/electrode interface, can be measured using GITT [6].

The objectives of the present work were to examine the charge/discharge of a cell using an amorphous V_2O_5 thin film deposited by r.f.-sputtering and to investigate the influence of Li content on the chemical diffusivity of Li ions in the amorphous V_2O_5 thin film using GITT.

S. Lee · J. Eom (✉) · H. Kwon
Department of Materials Science & Engineering, Korea
Advanced Institute of Science & Technology, 373-1,
Guseong-dong, Yuseong-gu, Daejeon 305-701, South Korea
e-mail: jyeom74@kaist.ac.kr

2 Experimental

V_2O_5 thin films were deposited on a p-type Si wafer and type 304 stainless steel by reactive r.f.-sputtering of a vanadium metal target 3 inches in diameter at $2\text{--}3\text{ W cm}^{-2}$ in a mixed gas environment of Ar + 40% O_2 . Total gas pressure was maintained at 10 mTorr during the reactive sputtering.

The charge/discharge experiments were performed using a cell which consisted of 1 M $LiClO_4$ -propylene carbonate (PC) solution as an electrolyte, the V_2O_5 thin film deposited on the stainless steel substrate as a working electrode, and Li metal as a reference and counter electrode. Charge/discharge experiments were performed in a potential range of 3.5 and 1.7 V at a constant current density of $50\text{ }\mu\text{A cm}^{-2}$. The Li ion diffusivity through the V_2O_5 thin film was measured at room temperature using GITT [6]. GITT consisted of immersing the working electrode in the same solution employed in the charge/discharge test, and then measuring an instantaneous potential change which was induced by applying a current pulse of $10\text{ }\mu\text{A cm}^{-2}$ to the working electrode. The current pulse which was applied for 60 s was then removed, and reapplied after the new equilibrium potential of the electrode was attained. By repeating these procedures, the Li ion diffusivity was determined in a potential range of 1.7–3.4 V.

The structure of the V_2O_5 thin film was characterized by X-ray diffraction (XRD), and its composition was analyzed by Auger electron spectroscopy (AES).

3 Results and discussion

3.1 Structure and composition of the V_2O_5 thin film

Figure 1a and b show the XRD results and the AES depth profile of the V_2O_5 thin film which was deposited at a thickness of 0.1 μm on the Si wafer. The XRD results indicated that the V_2O_5 thin film exhibited an amorphous structure because other peaks, with the exception of Si, were not observed. It is shown in Fig. 1b that the atomic ratio of O/V was about 2.3 which was less than the stoichiometric composition ($O/V = 2.5$) of V_2O_5 . This may have occurred due to the negative ion effect by which oxygen ions bonded loosely to the V_2O_5 thin film and were resputtered by O^- or O^{2-} negative ion particles moving quickly from the target to the substrate during the sputtering process [4]. Lourenco et al. reported that the oxygen gas ratio affected the composition of the amorphous V_2O_5 thin film, but the influence of the oxygen gas ratio on the V_2O_5 stoichiometry was small and the amorphous V_2O_5 thin film with a stoichiometric composition could not be

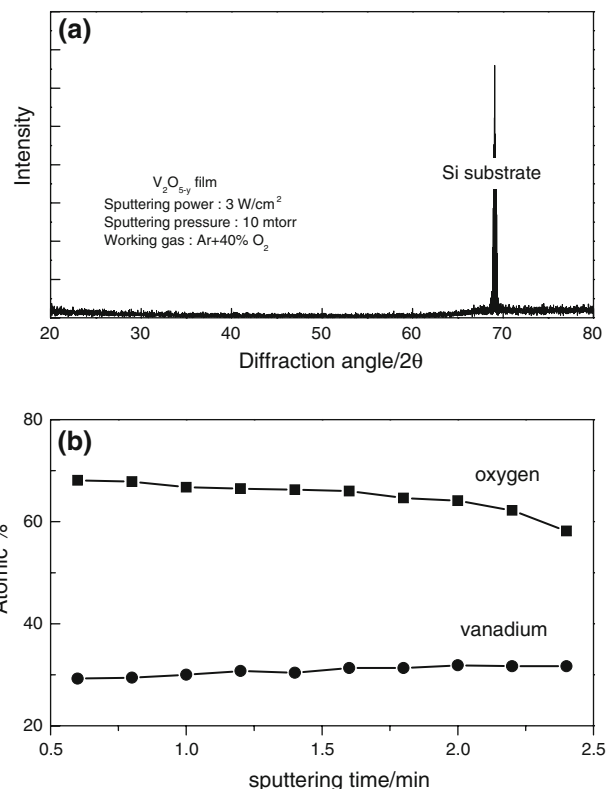


Fig. 1 (a) XRD pattern and (b) AES depth profile for V_2O_5 film deposited on Si substrate by r.f.-sputtering

obtained [12]. Thus, the actual composition of the thin film was regarded as V_2O_{5-y} .

3.2 Charge/discharge behavior of the V_2O_5 thin film

Figure 2 shows the first cycle curve of a charge/discharge for the $Li|1\text{ M }LiClO_4\text{-PC}|V_2O_{5-y}$ cell when the cell was discharged at $50\text{ }\mu\text{A cm}^{-2}$ from 3.5 to 1.7 V, then charged at the same current density to 3.5 V. The equilibrium potential of the V_2O_{5-y} electrode with respect to the Li electrode was measured to be 3.5 V. The intercalation of the Li ion into the V_2O_{5-y} cathode electrode which occurred during the discharge caused the chemical composition of the cathode to be changed to $Li_xV_2O_{5-y}$, with a simultaneous gradual change in electrode potential.

During the first discharge, the potential decreased gradually without exhibiting either a potential plateau or an abrupt potential reduction (Fig. 2). This appears to be characteristic in the charge/discharge curve of amorphous V_2O_{5-y} . In contrast, the charge/discharge curve of crystalline $Li_xV_2O_5$ has shown a step-type curve which alternated between a potential plateau and an abrupt potential reduction [2]. It was reported that the potential plateau was thought to result from the coexistence of two phases, and was observed at 3.4, 3.2 and 2.4 V for crystalline $Li_xV_2O_5$ [2].

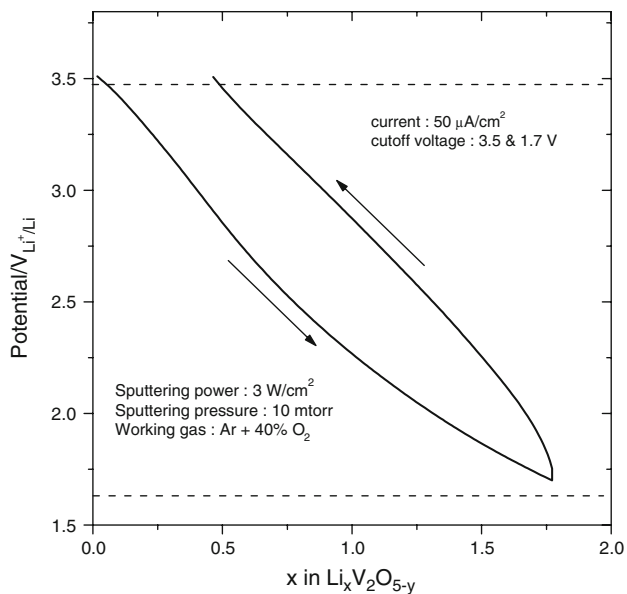


Fig. 2 First charge/discharge cycle of Li|1 M LiClO₄-PC|Li_xV₂O_{5-y} cell

The abrupt potential reduction was associated with the completion of phase transformation from δ phase to γ phase, which led to a capacity loss at the cathode due to an irreversible structural transformation [13].

The absence of a potential plateau and an abrupt potential reduction in the charge/discharge curve of the amorphous Li_xV₂O_{5-y} thin film suggests that the thin film maintained a single phase in the whole composition range ($x = 0-2.0$) without phase transformation during charge/discharge.

Figure 3 shows the discharge capacity of a cell as a function of the cycle number, measured at 300 $\mu\text{A cm}^{-2}$ and at a cutoff voltage between 1.7 and 3.5 V. The discharge capacity (Q) per unit volume of cathode can be calculated by dividing the charge which flowed during the discharge (from 3.5 to 1.7 V), by the volume of the cathode.

The discharge capacity at the first cycle was measured to be about 240 $\text{mC cm}^{-2}\text{-}\mu\text{m}$, and then decreased gradually with an increase in the number of cycles. When Q_n is the discharge capacity of the n th cycle and Q_0 is the discharge capacity of the first cycle, the reduction in the discharge capacity can be described by the power law ($Q_n = Q_0 \cdot (1 - \delta)^n$). δ is the relative capacity loss per cycle. In the case of the amorphous Li_xV₂O_{5-y} thin film cathode, δ was calculated to be 0.13% per cycle, showing excellent cycle performance.

3.3 Chemical diffusivity of Li ion in the V₂O₅ thin film measured using GITT

The cell reaction rate of the Li secondary battery was determined by the diffusion rate of the Li ion in the

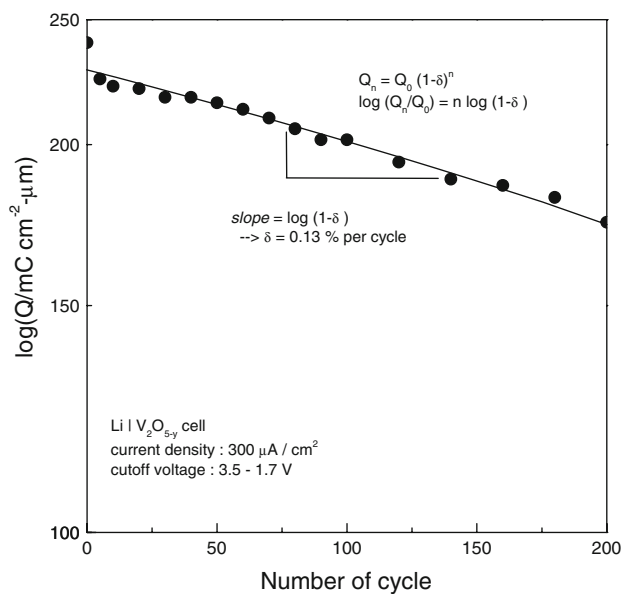


Fig. 3 The effects of cyclic number on the discharge capacity of Li|1 M LiClO₄-PC|Li_xV₂O_{5-y} cell

electrode as well as in the electrolyte. The rate determining step of the cell reaction was not the charge transfer reaction but the mass transfer reaction or diffusion of the Li ion [14]. In this work, chemical diffusivity of the Li ion in the amorphous V₂O_{5-y} cathode was investigated using GITT.

Determination of the Li ion diffusivity using GITT was carried out using the cell where the V₂O_{5-y} thin film and Li metal were used as a working electrode and a counter/reference electrode, respectively, in 1 M LiClO₄-PC solution. When the equilibrium potential (E_0) of a cell was reached, a current pulse of 10 $\mu\text{A cm}^{-2}$ for 60 s was applied to the cell and the resultant change in the electrode potential was measured simultaneously, as shown in Fig. 4.

During discharge at a constant current density of 10 $\mu\text{A cm}^{-2}$, Li ions intercalated into the cathode and a constant Li ion concentration gradient was formed at the electrolyte/cathode interface. The electrode potential decreased continuously to maintain a constant Li ion concentration gradient at the electrolyte/cathode interface. When the charge current was removed after τ (60 s), Li ions accumulated at the electrolyte/cathode interface and were uniformly distributed in the electrolyte and the cathode. When the electrode potential was increased slightly a new equilibrium state was established. The chemical diffusivity of a Li ion was obtained from Eq. 1 [10].

$$\tilde{D}_{\text{Li}^+} = \frac{4}{\pi} \left(\frac{V_m}{FS} \right)^2 \left[I_0 \left(\frac{\partial E}{\partial x} \right) / \frac{\partial E}{\partial \sqrt{t}} \right]^2 \text{ for } t \ll \frac{d^2}{\tilde{D}_{\text{Li}^+}}, \quad (1)$$

where \tilde{D}_{Li^+} is the chemical diffusivity of a Li ion, V_m is a molar volume of cathode and E is an electrode potential.

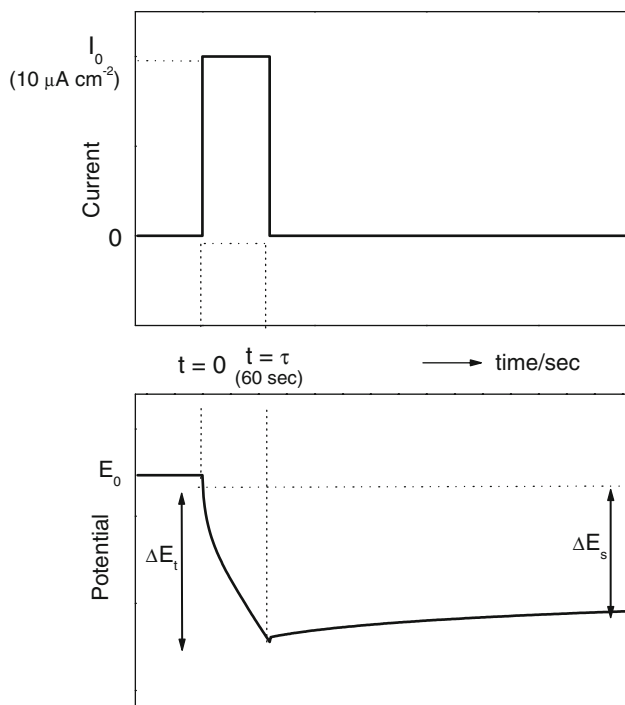


Fig. 4 Schematic illustration of a single step of GITT. ΔE_t is the total transient potential change in the galvanic cell for an current pulse of $10 \mu\text{A cm}^{-2}$ –60 s. ΔE_s is the change in the steady-state potential of the electrode for this step

The chemical diffusivity of a Li ion was calculated from Eq. 1 by applying the potential change with respect to a square root of time, $[(\partial E)/(\partial \sqrt{t})]$ and the potential change with respect to the content of Li, $[(\partial E)/(\partial x)]$ which was obtained from the change in the electrode potential in Fig. 5. The methods used to determine these values are described below using Figs. 5 and 6.

Figure 5 shows a plot of $E - E_0$ vs. \sqrt{t} at a discharge current of $10 \mu\text{A cm}^{-2}$ for 1 s, which was taken from the data in Fig. 4. The $E - E_0$ value decreased linearly with \sqrt{t} for 1 s after discharging, and the gradient of $[(\partial E)/(\partial \sqrt{t})]$ decreased with an increase in Li content.

Figure 6 shows the equilibrium electrode potential (or a coulometric titration curve) as a function of the Li content in the $\text{Li}_x\text{V}_2\text{O}_{5-y}$ cathode, which was obtained by applying GITT repeatedly in an electrode potential range between 3.5 and 1.7 V. From the curve in Fig. 7, the $[(\partial E)/(\partial x)]$ value was determined by obtaining E_0 and $E_0 + \Delta E$ at a Li content of, x and $x + \Delta x$, before and after applying the current pulse.

Figure 7 shows the chemical diffusivity of Li ions in the amorphous $\text{Li}_x\text{V}_2\text{O}_{5-y}$ thin film as a function of the Li content, which was calculated at room temperature using GITT. As the Li content in the cathode increased, the chemical diffusivity of Li ions decreased gradually from 4×10^{-13} to $7 \times 10^{-14} \text{ cm}^2 \text{ s}^{-1}$. These values for the

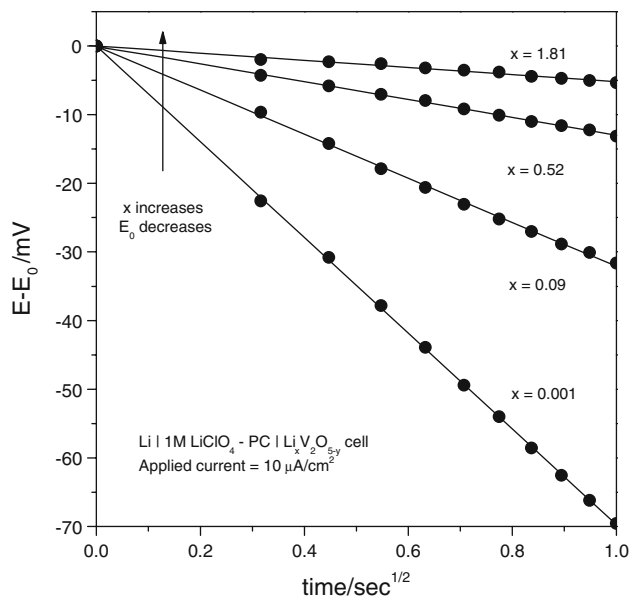


Fig. 5 Typical potential transient of $\text{Li}|1 \text{ M LiClO}_4\text{-PC}|\text{Li}_x\text{V}_2\text{O}_{5-y}$ cell as a function of the square root of the time

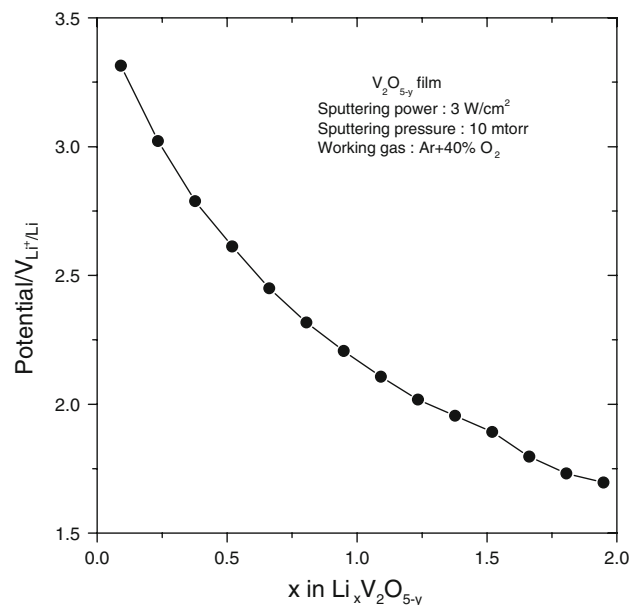


Fig. 6 The electrode potential transient of $\text{Li}|1 \text{ M LiClO}_4\text{-PC}|\text{V}_2\text{O}_{5-y}$ cell as a function of the Li content in $\text{Li}_x\text{V}_2\text{O}_{5-y}$

chemical diffusivity of Li ions was of the same order as those (10^{-13} – $10^{-14} \text{ cm}^2 \text{ s}^{-1}$ at 40°C) measured by the AC impedance method for $\text{Li}_x\text{V}_2\text{O}_5$ ($x = 0.5$ – 2) [15]. Figure 7 compares the chemical diffusivity of Li ions in the amorphous $\text{Li}_x\text{V}_2\text{O}_{5-y}$ thin film with those in the amorphous bulk $\text{Li}_x\text{V}_2\text{O}_5$ material made from amorphous $\beta\text{-V}_2\text{O}_5$ fabricated by the splat cooling method. As shown in Fig. 7, the chemical diffusivity of Li ions in the amorphous $\text{Li}_x\text{V}_2\text{O}_{5-y}$ thin film was 1–2 orders higher than that in the

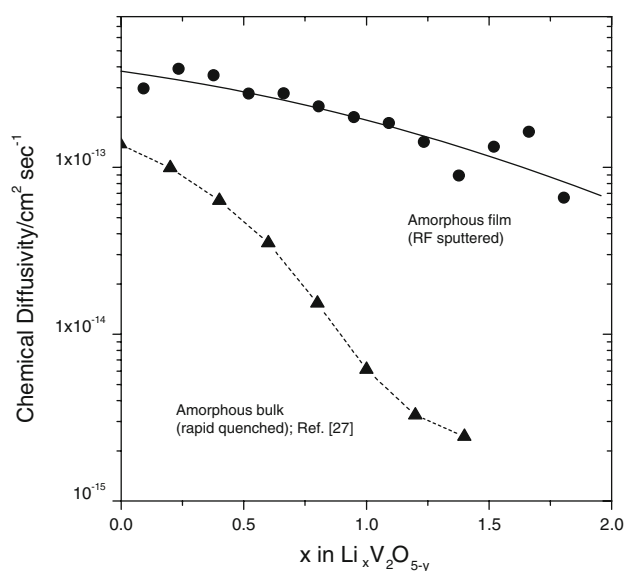


Fig. 7 The composition dependence of the chemical diffusivity (\bar{D}_{Li^+}) of the amorphous $\text{Li}_x\text{V}_2\text{O}_{5-y}$ thin film. The \bar{D}_{Li^+} of bulk amorphous $\text{Li}_x\text{V}_2\text{O}_{5-y}$ are shown for comparison

amorphous bulk material for a similar chemical composition [15]. This indicated that the amorphous bulk $\text{Li}_x\text{V}_2\text{O}_5$ has a structural property of $\beta\text{-V}_2\text{O}_5$ which had a low chemical diffusivity ($10^{-15} \text{ cm}^2 \text{ s}^{-1}$) for Li ions.

4 Conclusions

1. The V_2O_5 thin films deposited using reactive r.f.-sputtering of a vanadium target in $\text{Ar} + 40\% \text{ O}_2$ exhibited an amorphous structure with a chemical composition of V_2O_{5-y} ($y \approx 0.4$).
2. The absence of a potential plateau and an abrupt potential reduction in the charge/discharge curve of the $\text{Li}|1 \text{ M LiClO}_4\text{-PC}| \text{V}_2\text{O}_{5-y}$ thin film cell demonstrated that the $\text{Li}_x\text{V}_2\text{O}_{5-y}$ thin film electrode maintained a single phase during the charging/discharging process without phase transformation.

3. The discharge capacity of the $\text{Li}|1 \text{ M LiClO}_4\text{-PC}| \text{V}_2\text{O}_{5-y}$ thin film cell was about $240 \text{ mC cm}^{-2}\text{-}\mu\text{m}$ at the first cycle, and gradually decreased with an increase in the number of cycles to 0.13% per cycle at 200 cycles, showing excellent cycle performance.
4. The chemical diffusivity of Li ions in the amorphous $\text{Li}_x\text{V}_2\text{O}_{5-y}$ thin film, measured by GITT, decreased from 4×10^{-13} to $7 \times 10^{-14} \text{ cm}^2 \text{ s}^{-1}$ with Li content (x).

Acknowledgements This work was supported by the Growth Engine Technology Development Program (Project No. 10016472) and the BK21 program funded by Korea Ministry of Knowledge Economy.

References

1. Besenhard JO (1999) Handbook of battery materials. Wiley-VCH, Weinheim
2. Dickens PG, French SJ, Hight AT et al (1979) Mater Res Bull 14:1295
3. Cartier C, Tranchant A, Verdaguer M et al (1990) Electrochem Acta 35:889
4. West K, Christiansen BZ, Skaarup SV (1992) Solid State Ionics 57:41
5. Bates J, Gruzalski GR, Bates NJ et al (1994) Solid State Ionics 70/71:619
6. Weppner W, Huggins RA (1977) J Electrochem Soc 124:1569
7. Bae JS, Pyun SI (1995) J Alloys Compd 217:52
8. Leroux F, Koene BE, Nazar LF (1996) J Electrochem Soc 143:181
9. Lee DB, Passerini S, Guo J et al (1996) J Electrochem Soc 143:2099
10. Thompson AH (1979) J Electrochem Soc 126:608
11. Ho C, Raistrick ID, Huggins RA (1980) J Electrochem Soc 127:343
12. Lourenco A, Gorenstein A, Passerini S et al (1996) J Electrochem Soc 145:706
13. Tranchant A, Blengino JM, Farcy J et al (1988) Electrochim Acta 33:1003
14. Machida N, Fuchida R, Minami T (1989) J Electrochem Soc 136:2133
15. Kumagai N, Kitamoto H, Baba M et al (1998) J Appl Electrochem 28:41